Large Strain Hysteresis and Mullins Effect of Tough Double-Network Hydrogels

Rebecca E. Webber and Costantino Creton*

Laboratoire de Physico-Chimie des Polymères et Milieux Dispersés, UMR 7615 CNRS−UPMC-ESPCI, 10, Rue Vauquelin, Paris, France

Hugh R. Brown

Faculty of Engineering, University of Wollongong, Wollongong, NSW 2522, Australia

Jian Ping Gong

Laboratory of Soft and Wet Matter, Department of Biological Sciences, University of Hokkaido, Japan

Received December 20, 2006; Revised Manuscript Received February 7, 2007

ABSTRACT: Systematic loading and unloading experiments, in uniaxial tension and uniaxial compression, have been performed on a double-network hydrogel exhibiting a very high toughness. We observed a significant hysteresis during the first loading cycle that increased strongly with the applied maximum deformation. A large hysteresis was not observed during a second loading cycle, implying that the initial hysteresis can be attributed to the fracture of covalent bonds in the primary network. We report this type of dissipative mechanism for polymer gels for the first time. Assuming that the entire energy dissipated during the hysteresis cycle can be attributed to the fracture of network strands by a Lake−Thomas mechanism, our results suggest that the fracture and unloading of only 1% of the bonds within the network leads to a decrease of up to 80% of the number of strands. These results also demonstrate the very large degree of heterogeneity within the hydrogel network. If such a dissipative mechanism is active at the crack tip, it will most likely greatly increase the energy necessary to propagate a macroscopic crack, elucidating the origin of the toughness in these interesting materials.

Introduction

With their high water content and carbon-based network structure, hydrogels are the closest synthetic approximation to biological tissue and materials. Hydrogels are particularly interesting due their potential in a myriad of applications, ranging from drug delivery[1] to artificial cartilage[2,3] in the realm of biological sciences and including superabsorbants,[4] microfuidics,[5] and contact lenses[6] in the materials science domain.

Because the first generation of hydrogels was mechanically weak, there was not much interest in extensively investigating the origin of their mechanical properties. They were universally understood to be weak systems due to the high water content and the stretched and swollen state of the polymer chains. However, while synthetic hydrogels are generally rather fragile materials, those found in nature are much tougher. Newer classes of hydrogels currently under investigation are those possessing a greater degree of toughness, or fracture resistance, more similar to natural systems. These hydrogels generally have a more complex structure, and interest in understanding the mechanical properties of these materials has resurfaced. The new class of tough hydrogels includes double network (DN) gels,[7−9] nanocomposite gels,[10] natural polymer gels,[11,12] and interpenetrating network gels.[13]

The mechanical behavior of these systems approaches that of the behavior of a classical elastomer, but the typical rubber elasticity models, such as Mooney−Rivlin, Gent,[14] and Edwards and Vilgis,[15] do not seem to adequately explain their properties at large strain. Polyelectrolyte gels, a common example, have long posed problems for these models, although their swelling behavior has been extensively studied.[16−18] While inhomogeneity plays a role in controlling the unique mechanical properties of these systems, it is not the complete story, nor is it true in every case.[9,19−21]

Understanding what makes these new gels tough has been a recent challenge. These materials are not only fundamentally interesting but also useful in a variety of potential applications that require adequate mechanical performance at stresses of above ∼10 MPa. Specific examples include artificial cartilage and ligaments and more ergonomic prosthetics.[9] We are particularly interested in the double network (DN) gels introduced by the Gong group. The DN gels possess exceptional mechanical properties, including a high fracture strength (17.2 MPa in compression and 0.68 MPa in tension) and a large fracture strain (92% and 75% in compression and tension, respectively).[8] Although containing only 10 wt % polymer, they behave as robustly as some solvent-free conventional elastomers. These characteristics have far-reaching implications for the applications mentioned above as well as for an understanding of material behavior in general. Fully understanding the source of these systems' exceptional mechanical strength could be essential for the design of future synthetic gels.

Theoretical Considerations

Double-network gels have a very high toughness compared to normal single-network gels. On the basis of previous work on these materials,[8,9,20] it is known that this enhancement in toughness is particularly significant when the first network is heterogeneous and brittle, in other words charged and highly cross-linked, and the second network is soft and weakly cross-linked. In general, if macroscopic crack propagation occurs, a high material toughness is associated with a dissipative mech-

* To whom correspondence should be addressed. E-mail: costantino.creton@espci.fr.

10.1021/ma062924y CCC: $37.00
Published on Web 03/21/2007

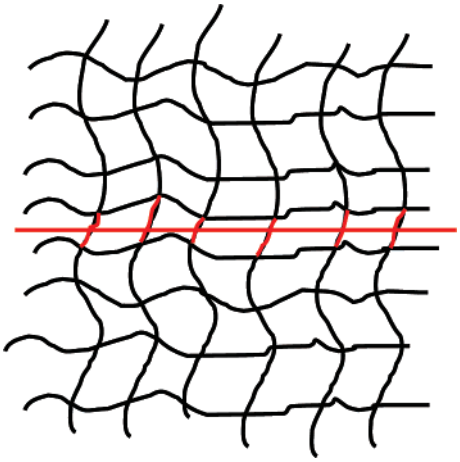

Figure 1. Schematic of fracture of network strands along a plane.

anism around the crack tip.[22] In the present study, we focus on identifying the molecular origin of this dissipative mechanism. The fracture experiments of Gong et al., performed at different crack propagation rates, show little or no velocity dependence.[9] Similar experiments performed in our lab support these results. This observation implies that no viscous dissipative mechanism is at work during the fracture process and that the most likely dissipative mechanism is the sudden release of energy due to bond breakage.

In principle, the minimum amount of energy that can be released during bond breakage is the energy of the bond itself. However, this would significantly underestimate the measured value of energy lost, even in the complete absence of viscoelastic dissipation. This minimum amount of energy is called the fatigue threshold of a rubber and only depends on the architecture of its network. The underlying mechanism was proposed more than 40 years ago and is known as the Lake−Thomas effect.[23] In essence, the breakage of each network strand between two cross-link points irreversibly dissipates the strain energy of each monomer composing the strand, which is assumed to be stretched to the same level as the broken bond. This leads to an amplification factor on the order of the number of monomers per network strand.

During the propagation of a crack along a given fracture path, if we assume that all the network strands within this path are broken and that the path is planar, the energy dissipated per unit area is simply the areal density of network strands crossing the plane of fracture, Σ, times the average number of monomers composing each strand, as described two-dimensionally in Figure 1. If the network is homogeneous, the fracture of each strand dissipates an energy equal to $\bar{N}_c U_b$, where $\bar{N}_c$ is the average number of C−C bonds between two cross-links and U_b is the energy of a covalent carbon−carbon bond. If we assume that N_c is ∼20 and U_b is 360 kJ/mol, the fracture energy is then 7200 kJ/mol. The areal density of strands within a plane can be estimated from the length of a strand. For a single network poly(2-acrylamido-2-methylpropanesulfonic acid) (PAMPS) gel, which is highly charged and therefore highly extended, we can assume that the length of a strand of 10 monomers is ∼3.5 nm (0.75 × 0.5 nm × 10), making the areal density $\sim 8 \times 10^{16}$ m^{-2}. The fracture energy is then $\bar{N}_c U_b \Sigma / N_A = 1$ J/m^2.

Real networks however are typically heterogeneous in terms of their cross-linking structure and may resemble the structure shown in the schematic in Figure 2 with less cross-linked regions connected by more cross-linked regions. While everyone agrees on the heterogeneous nature of the gels' structure, the details

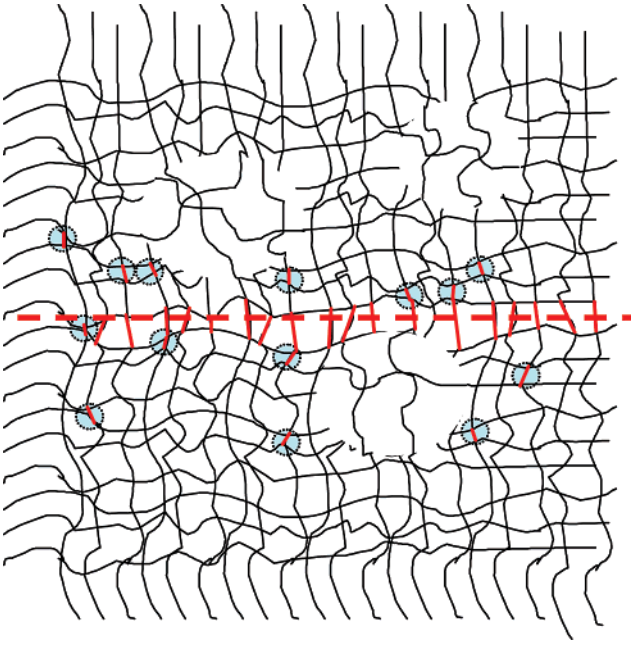

Figure 2. Schematic of a heterogeneous network, with the dashed line representing the plane of fracture and circles showing the short strands of preferential covalent bond fracture away from that plane.

of that structure remain a matter of debate. Much depends on the individual system and synthesis conditions.[21,24,25] If a crack propagates through such a structure, it is likely that the fracture of short strands in the highly cross-linked regions distributed throughout the volume of the network will occur over a three-dimensional volume rather than being confined to a plane, as shown in Figure 2, making the amount of energy dissipated potentially much larger.

For this situation to occur, there are two necessary conditions. The first condition is that the cross-linking must be highly heterogeneous, creating a network in which short strands (reaching their extensibility limit) break first and far from the crack tip. The second condition is that the fracture of short strands must not lead to macroscopic crack propagation via the coalescence of microscopic cracks. This second condition forms the basis of a recently proposed model of gel fracture for double-network gels.[26] The model suggests that the second network in DN gels serves to redistribute the stress concentration in a way similar to that of craze formation in a glassy polymer, thereby avoiding crack propagation. This process causes a large damage zone and increases the toughness of the DN gel by a factor of about 50 over the toughness of the second (tough) network.

In the present paper we investigate the hypothesis that fracture in DN gels involves the breakage of a large number of load-bearing strands that are distributed over a volume.

As in most toughening mechanisms of polymers, this scenario implies that some microscopic fracture event must occur in the material before macroscopic failure occurs. This type of fracture event should be mechanically detectable, through the presence of a hysteresis in the loading−unloading curve. It is important to note that, in the DN gels, viscoelastic hysteresis is likely to be negligible because of the low viscosity of the medium. In this work, we have performed systematic loading−unloading experiments on the DN gels at increasing levels of strain in both simple compression and simple tension. In recording the level of hysteresis during these experiments, we investigate the heterogeneous structure of the gel network.

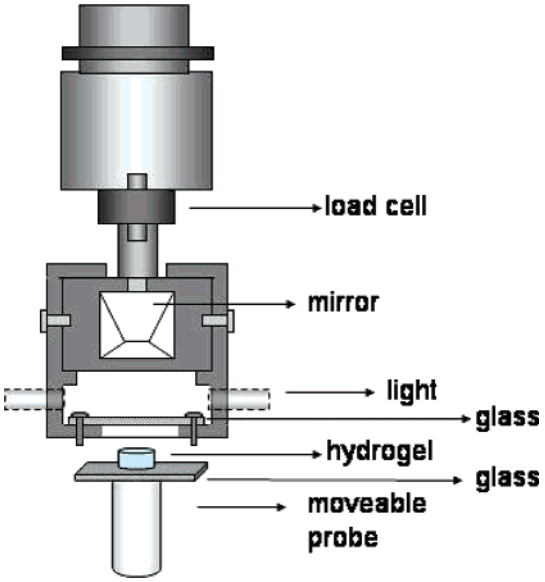

Figure 3. Compression test apparatus.

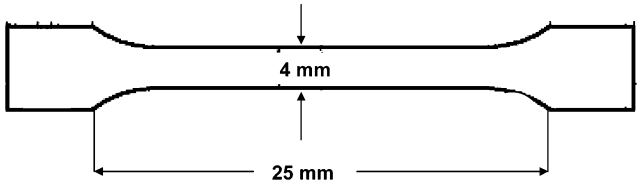

Figure 4. Geometry of tensile test sample.

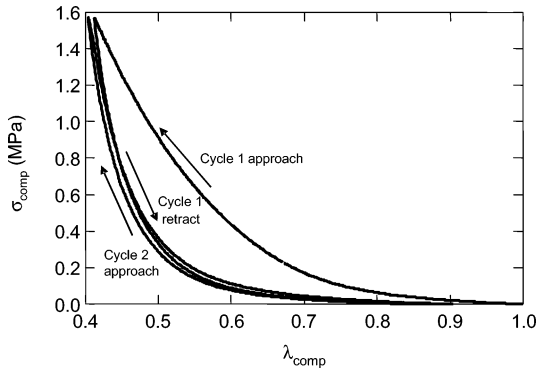

Figure 5. Compressive stress vs compressive lambda curves from a typical two-cycle compression experiment.

Experimental Section

Materials. The DN hydrogels used in this work were synthesized via a two-step sequential UV polymerization technique.[8,9] The first network was prepared from a 1 M aqueous solution of 2-acrylamido-2-methylpropanesulfonic acid (AMPS) with 4 mol % *N*,*N*′-methylenebis(acrylamide) (MBAA) as a cross-linker. The gel obtained after UV polymerization was immersed in a 2 M solution of acrylamide and allowed to swell to equilibrium. The second (uncross-linked) network was then synthesized by the same procedure around the first swollen network. The initiator for both reactions was 0.1 mol % (relative to monomer) α-ketoglutaric acid. This procedure results in a gel composed of two interpenetrating, swollen networks; the molar ratio of the second network to the first is 20. The DN gel was then allowed to swell in deionized water until equilibrium, decreasing the total polymer concentration to about 10%. Details of the hydrogel preparation have been described previously.[8,9] Double-network hydrogels prepared in this way were stored at ambient temperature in water between experiments. Appropriately shaped samples for rheology, compression, and tension experiments were cut using sharpened punches and a press.

Mechanical Testing. *Compression.* Cyclic compression experiments were performed on an MTS tensile test machine using a 50 N load cell (Sensotec). The hydrogel, in the form of a cylinder (∼5 mm diameter and 3 mm in initial thickness), was placed on a glass slide and brought into contact with a second glass surface to a point of maximum compression before being retracted back to zero load. Load and displacement data were collected during the experiment, and the contact area and form of the gel were visually monitored via a mirror throughout. In this way we could clearly see that slippage occurs at the interface and that the gel deforms at constant macroscopic volume and with an essentially full-slip boundary condition. With these experiments, we are, in effect, performing a uniaxial compression test equivalent to biaxial deformation in the plane normal to the loading direction. Figure 3 shows a schematic of this test setup.

Tension. Tension experiments were performed using a JFC TC3 tensile test machine. Samples were cut to the requirements shown in Figure 4 and held on the machine between clamps altered with wood strips to better grip the slippery materials. A typical tensile test consisted of an imposed traction to a set maximum displacement followed by a return to zero load. Cyclic tests were performed by performing subsequent trials immediately following the initial loading.

Results

Compression. In this work, a typical compression test consists of initial compressive contact to 0.5 N followed by retraction to 0.01 N to ensure a starting point of complete contact between the gel and glass surfaces. The test then begins with a compression step performed at a constant crosshead speed of 25 μm/s (corresponding to an initial strain rate of 0.86×10^{-2} s^{-1}) to a maximum load (varied between 5 and 45 N), followed by immediate retraction to 0.01 N and a wait time, usually 30 s, until the next cycle of compression. Figure 5 shows a typical stress−lambda curve from a compression test trial composed of two cycles of compression to 25 N. Compressive stress is positive in the following discussions because we will be regarding compression as biaxial extension, as outlined below. The stress is nominal, defined as $\sigma_{comp} = P/\pi a_0^2$, where P is the experimental force and a_0 is the initial radius of the gel cylinder. The parameter lambda is defined as $\lambda = h/h_0$, where h_0 is the initial height of the gel cylinder and h is its current height.

All compression tests were performed on fresh samples so that the term "first compressive cycle" always refers to a sample that has not been previously deformed. In all cases the loading curve of the first compressive cycle is different from the unloading curve and equally different from the second loading curve. As can be seen from Figure 5, the second loading/unloading cycle is nearly elastic and closely follows the path of the first unloading.

This behavior is very similar to the so-called "Mullins effect" observed for filled rubbers. However, there are two significant differences that relate to recoverability and second-cycle hysteresis. In filled rubbers, the behavior of the virgin sample can be recovered when the sample is left to rest without stress; typically within 1 h, a new "first compression" curve can be obtained, suggesting a slowly relaxing deformation mechanism. In the case of DN hydrogels, we have waited up to 1 week without having any substantial recovery of the virgin behavior. The hysteresis of the second cycle in rubbers is still rather substantial due to molecular friction. In our case the hysteresis of the second cycle is barely measurable, implying very little dissipation at the molecular level.

The irrecoverable nature of the damage done to the gel during the first loading cycle is illustrated in Figure 6, showing successive loadings of the same gel sample. A first loading cycle

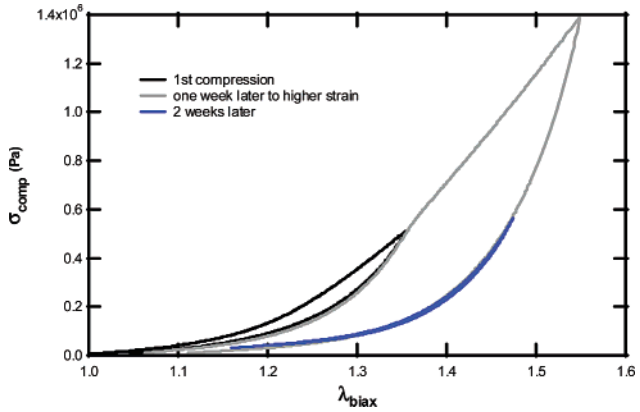

Figure 6. Successive loading cycles in compression of the same gel sample.

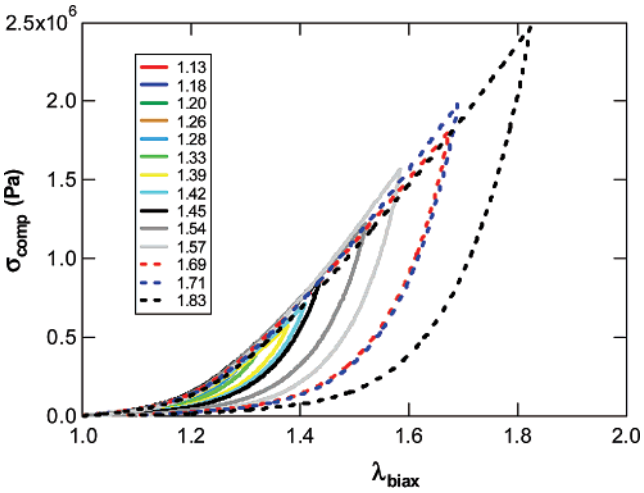

Figure 7. Typical stress−lambda curves for the first compressive cycle as a function of increasing strain (virgin samples). Values in the legend correspond to the maximum values of λ_{biax} achieved for each test.

was performed to a maximum λ_{biax} of 1.35; after 1 week, during which the sample was kept in water, a second loading cycle was carried out to about $\lambda_{biax} = 1.55$, and Figure 6 shows that the loading curve closely follows the unloading curve of cycle 1 up to $\lambda_{biax} = 1.35$ but appears to continue the loading curve of cycle 1 for $\lambda_{biax} > 1.35$. Finally, a third loading to $\lambda_{biax} = 1.48$ was carried out on the same sample after an additional week, and in this case, the loading curve closely follows the unloading curve of cycle 2, clearly demonstrating the irreversibility of the damage done to the gel in the previous loading cycles. The number of fracture events is therefore directly dependent on the maximum strain achieved during the first cycle; i.e., if a second loading−unloading cycle is performed at a lower or equivalent maximum strain, the material behaves very elastically. On the other hand, if the maximum strain of the second cycle surpasses that of the first cycle, the loading curve has two parts, as shown in Figure 6.

In order to systematically investigate these fracture events, each virgin sample was compressed once to a certain level of applied force and then unloaded and immediately reloaded a second time. Figure 7 displays a series, in increasing maximum lambda ($\lambda_{biax,max}$), of typical stress−lambda curves for the first cycle of compression. Since uniaxial compression is equivalent to biaxial stretching in terms of deformation, we have used

$$\lambda_{biax} = \frac{1}{\sqrt{\lambda_{com}}} \qquad (1)$$

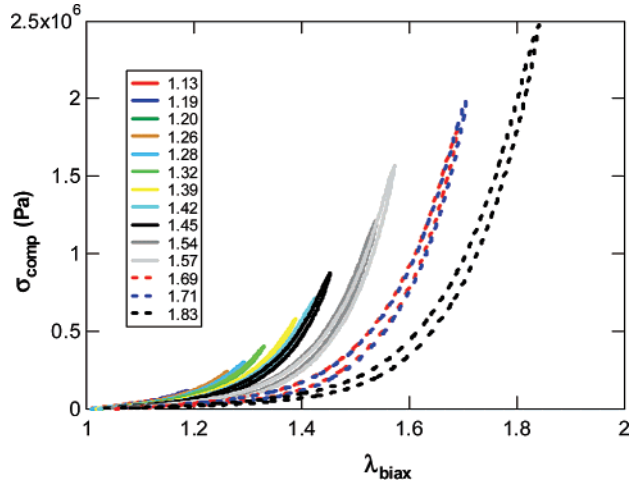

Figure 8. Series of stress−lambda curves for the second compressive cycles.

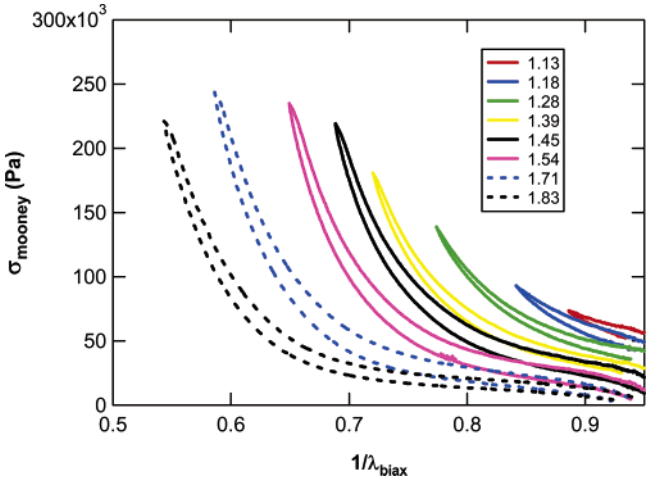

Figure 9. Mooney representation of curves from the second compressive cycles.

as our deformation variable to provide an easy comparison with uniaxial stretching, which is presented later.

It is clear that while the loading curves fall on the same master curve, the unloading curves are all different, strongly suggesting that the hysteresis observed in the first cycle is related to irreversible fracture events taking place for different values of $\lambda_{biax,max}$. The stress−lambda curves for the series of second compressive cycles are shown in Figure 8 (for different values of maximum first cycle λ). These cycles were performed immediately after the first compressive cycles shown in Figure 7.

In all cases, the DN gels behave elastically during the second loading, with a very limited hysteresis. It is also clear, however, that the DN gels display a significant degree of strain hardening in these second loading curves. In order to emphasize this nonlinear elastic behavior, it is more convenient to use the Mooney stress representation classically used for rubbers. The Mooney stress, defined below, can be typically plotted as a function of $1/\lambda_{biax}$:

$$\sigma_{Mooney} = \frac{\sigma_{comp}}{\lambda_{comp} - \frac{1}{\lambda_{comp}^2}} = \frac{\sigma_{comp}}{\lambda_{biax}^4 - \frac{1}{\lambda_{biax}^2}} \qquad (2)$$

The Mooney representation of the second compressive cycles is shown in Figure 9 for the maximum lambda series introduced above.

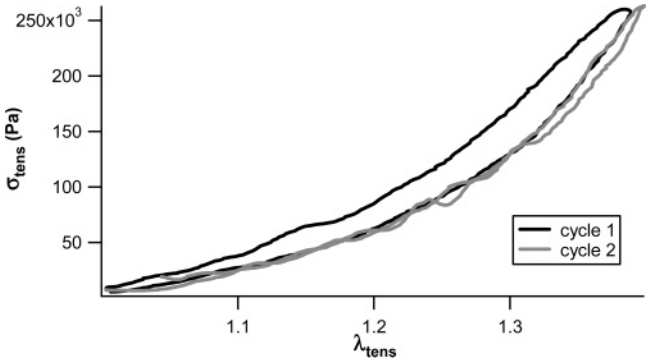

Figure 10. Stress−lambda plot for subsequent cycles of a tensile experiment.

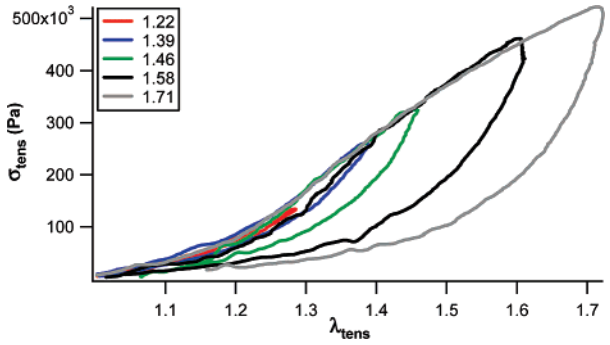

Figure 11. Stress−lambda curves as a function of maximum lambda for the first cycle of a series of tensile tests.

From Figure 9, it is evident that for increasing λ_{max} the Mooney stress is smaller at small strains and that strain hardening begins at higher strains. It is also clear that the small strain modulus of the hydrogels, directly represented by the Mooney stress at values of λ close to one, decreases with increased compression during the first cycle.

Tension. Since it has recently been reported[27] that the tensile behavior of some DN gels can be significantly different from the compressive, or biaxial stretching, behavior of these materials, we also performed tensile experiments on the DN gels.

Figure 10 shows subsequent cycles of typical tensile stress−lambda curves for a 1.7 mm thick sample. The stress is nominal, defined as $\sigma_{tens} = P/tw$, where P is the experimental force and t and w are the original thickness (~2 mm) and width (4 mm) of the gel sample, respectively. The value lambda is defined as $\lambda_{tens} = h/h_0$, where h_0 is the initial gage length of the gel sample (25 mm) and h is its current length.

We carried out the same series of systematic loading−unloading experiments in tension, to a maximum strain value ($\lambda_{tens,max}$), that were described earlier in compression. The main observations from these trials were the following:

(i) As in the compression experiments, a significant hysteresis was observed for the first loading cycle. This is shown in Figure 11 for a series of samples stretched to different values of $\lambda_{tens,max}$. Higher extensions resulted in larger observed hystereses. Unlike the experiments of Na et al.,[27] these gels never formed a necked region during extension, but the beginning of a softening process suggests that this may have happened at higher strain values.

(ii) The first cycles from both tension and compression are plotted together on Figure 12 in the Mooney representation.

Interestingly, this representation highlights the fact that, in the first loading, these gels do show a hardening followed by a stabilization of the modulus, a very peculiar behaviour for a network, suggesting a yielding mechanism.

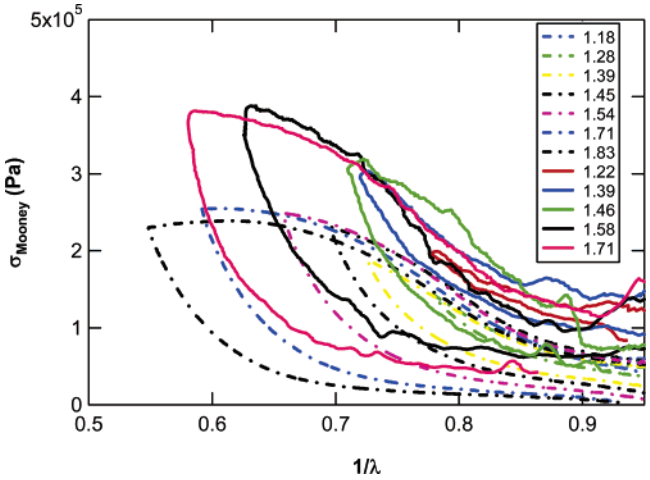

Figure 12. Loading and unloading curves for the first cycle in tension (full lines) and in compression (dotted lines) for different values of maximum lambda (λ_{tens} and λ_{biax}, respectively).

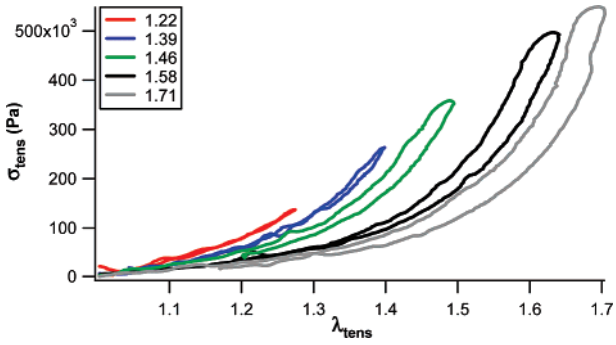

Figure 13. Stress−lambda curves as a function of first-cycle maximum lambda for the second cycle of a series of tensile tests.

Similar to the observed behavior in compression, the second tensile loading was very elastic with a minimum amount of hysteresis, as shown in Figure 13. However the amount of hysteresis observed during the second loading was slightly larger in tension than in compression.

Analysis. It is clear from the data presented above that the DN gels have a very peculiar behavior in large strain, with a very large first cycle hysteresis and a very elastic second cycle behavior that is dependent on the level of deformation reached during the first cycle. In this section, we attempt a more quantitative analysis of the data, beginning with a more quantitative analysis of the hysteresis of the first loading cycle.

The hysteresis, or energy dissipated, is calculated according to the following equation:

$$U_{hyst} = \frac{1}{h_0}\int_{loading}\sigma\, d\delta - \int_{unloading}\sigma\, d\delta \qquad (3)$$

If we assume that no viscous dissipation is involved in creating the first-cycle hysteresis, that all dissipation is due to bond fracture, and that the Lake−Thomas model applies for all broken load-bearing strands, we can estimate the fraction ϕ_b of covalent bonds actually broken or "unloaded" by the fracture process according to

$$\phi_b = \frac{U_{hyst}}{C_{C-C}U_b} \qquad (4)$$

where C_{C-C} (120 mol/m^3) is the molar concentration of C−C bonds in the primary network and U_b (360 kJ/mol) is the fracture energy of a C−C bond. Numerical values obtained from the

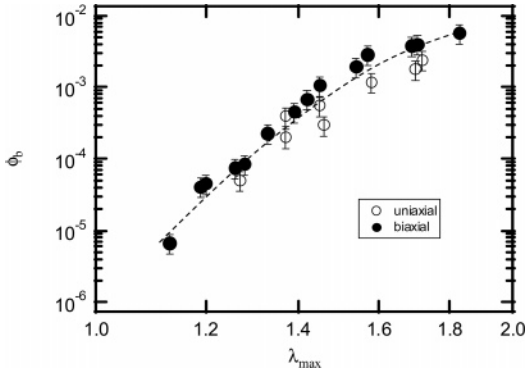

Figure 14. Fraction of bonds that are "destressed" during the first loading cycle as a function of maximum lambda. The dashed line is a guide to the eye.

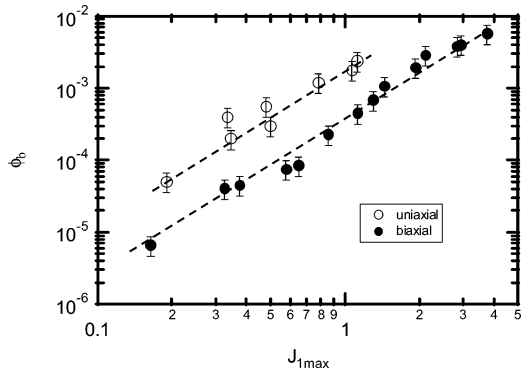

Figure 15. Fraction of bonds that are "destressed" during the first compressive loading cycle as a function of the first strain invariant J_1.

compression and tension experiments are reported in Figure 14 as a function of the maximum strain (biaxial or uniaxial) achieved during the first cycle. The physical interpretation of the data is that ϕ_b is the fraction of covalent bonds in the primary network that have become unstressed, either broken or no longer load bearing, during the deformation process.

This fraction of unloaded bonds from Figure 14 can then be related to the structure of the partially fractured network, which can be characterized from the second loading cycle.

It is apparent that as the maximum extension during the first cycle increases, the level of hysteresis upon unloading increases. If this hysteresis is attributed solely to the energy loss by the Lake−Thomas mechanism during the fracture of the strands, the hysteresis can be directly related to the fraction of unloaded monomers. It is interesting to note that the absolute values of the fraction of broken bonds remain below 1% in these experiments but still has a significant impact on the elastic properties of the material during the second loading, as can be seen by comparing Figures 11 and 13, for example. Another interesting observation can be made by looking more closely at Figure 14. The fraction ϕ_b only depends on the maximum value of λ and not on a more general measure of the strain state such as the first strain invariant J_1 defined as

$$J_1 = \lambda_1^2 + \lambda_2^2 + \lambda_3^2 - 3 \tag{5}$$

When the same values of ϕ_b are plotted in Figure 15 as a function of the maximum value of the strain invariant achieved during the first loading cycle, it is clear that this is not the parameter controlling the fraction of broken bonds.

In order to estimate the change in properties of the network after strands have been broken, we can calculate the variation in the Mooney stress at a moderate strain ($\lambda = 1.1$) between

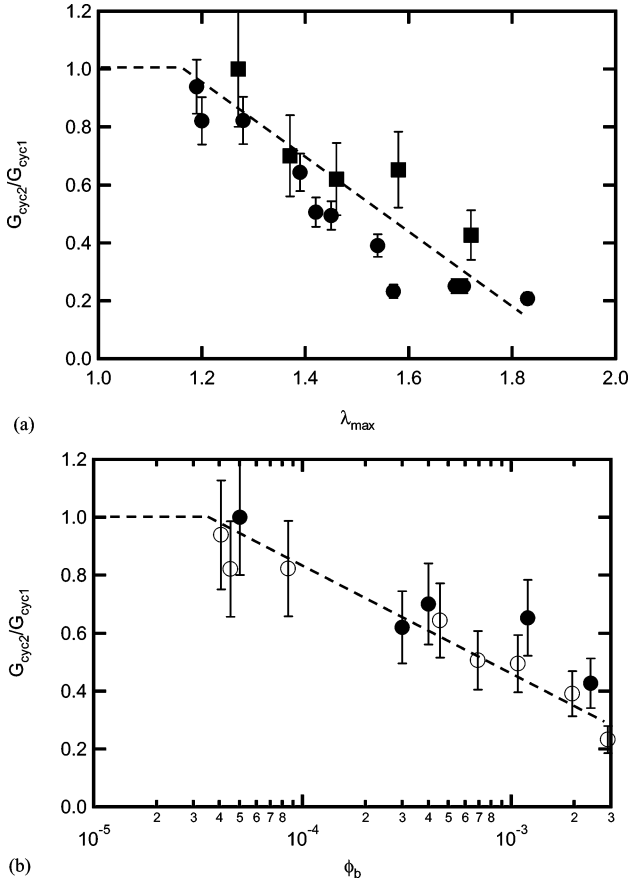

Figure 16. Fractional loss in modulus (a) as a function of the maximum biaxial extension achieved in the first loading and (b) as a function of the fraction of unloaded bonds.

the first and second cycles. This change in Mooney stress can be related to the decrease in the number of available elastic strands per unit volume using classical Gaussian rubber elasticity.

Figure 16a shows the change in Mooney stress (equivalent to the small strain shear modulus G) between the two cycles as a function of λ_{max} in the form of a fraction of the original modulus (G_{cyc2}/G_{cyc1}), where G_{cyc1} is the value of the Mooney stress calculated during compression cycle 1 and G_{cyc2} is the same modulus for cycle 2. Data from compression and tension experiments are compared directly in Figure 16a, and despite the difference between biaxial and uniaxial stretching, the trends are quite clear. Above $\lambda_{max} = 1.2$, we see a clear decrease in the modulus between cycles. This is the threshold strain at which a significant number of short strands that contribute to the material stiffness in the first network begin to break.

When G_{cyc2}/G_{cyc1} is plotted vs ϕ_b (Figure 16b), it is clear that the small strain modulus decreases significantly (20% of the original value) when the network is strained to values of λ_{max} equal to approximately 1.6−1.8, while the observed hysteresis is only equal to about 1% of the binding energy of the C−C bonds of the first network. Although there are some variations from sample to sample, the shear modulus drops from approximately 80 to 15 kPa for the most damaged network.

Several molecular interpretations of this result, which depend on the approximations made, can now be discussed. The most straightforward interpretation of the modulus of a cross-linked gel is to assume that

$$G = \frac{1}{2}\nu kT \tag{6}$$

where υ is the number of cross-links per unit volume. This implies that a decrease in G of 80% would correspond to 80% of the strands of the first network being broken. There are then two limiting cases for the molecular interpretation of the hysteresis. If we assume that the dissipated energy is due only to the broken bonds themselves, then fracturing 1% of the bonds corresponds to breaking 25% of the first network gel strands (keeping in mind that the gels contain 4 mol % of cross-linker), which would imply a moderate level of heterogeneity. However, if we assume that each broken bond actually unloads all monomers in its strand and that this energy is irreversibly lost, then 80% of the strands only contain less than 1% of the bonds. Using this interpretation, the results shown in Figure 14 are a signature of the very large degree of heterogeneity of the first network. In essence, less than 1% of the AMPS monomers are located in 80% of the strands. If we make the analogy with the molecular weight distribution of a linear polymer, then the polydispersity of M_c is extremely large. This result is consistent with the nonlinear behavior of the DN gels, which never shows any real Gaussian elasticity (a nearly constant value of Mooney stress) until a significant number of these short bonds are broken. This is also consistent with the extremely high modulus measured on the unbroken network. The measured shear modulus of ~80 kPa would correspond to ~65 mol/m^3 of elastic strands if they were Gaussian. In reality, even a perfect first network cannot contain more than 5 mol/m^3 of strands on average. Therefore, the modulus of the virgin material is very much dominated by the short, highly extended PAMPS strands.

Finally, in terms of nonlinear elasticity, Figure 9 shows that the onset of strain hardening occurs later as the maximum biaxial deformation increases. This is a clear indication that the shortest strands are being broken first, allowing the extension of longer PAMPS strands.

We can try to analyze this trend more quantitatively by using a simple nonlinear elastic constitutive equation which includes strain hardening. In a relatively recent paper, Gent proposed a simple model for unentangled cross-linked networks undergoing strain hardening at large strains.[14] He proposed the following expression for the elastic strain energy per unit volume:

$$W = -\frac{G}{2} J_m \ln\left(1 - \frac{J_1}{J_m}\right) \tag{7}$$

where G is the shear modulus, J_1 is the first stress invariant for simple extension in the 1-direction (equal to $\lambda_1^2 + 2\lambda_1^{-1} - 3$), λ_1 is the principal stretch ratio in the 1-direction (λ_{comp} or λ_{tens} in our tests), and J_m is an adjustable parameter representing finite extensibility as a maximum allowable value for the first stress invariant. This constitutive equation and eq 1 can be used to predict the tensile or compressive stress as a function of λ_{tens} or of λ_{biax} with two adjustable parameters, G and J_m:

$$\sigma_{tens} = G \frac{\lambda_{tens} - \lambda_{tens}^{-2}}{1 - (J_1/J_m)} \tag{8a}$$

$$\sigma_{comp} = G \frac{\lambda_{biax}^{4} - \lambda_{biax}^{-2}}{1 - (J_1/J_m)} \tag{8b}$$

Two representative fits of the compression data are shown in Figure 17. Equation 8b fits the strain hardening of the second loading of the DN hydrogels fairly well. However, because the measured strain hardening for the most damaged networks was more abrupt than eq 8b could predict, our fits attribute greater weight to the large strain portion and the J_m parameter.

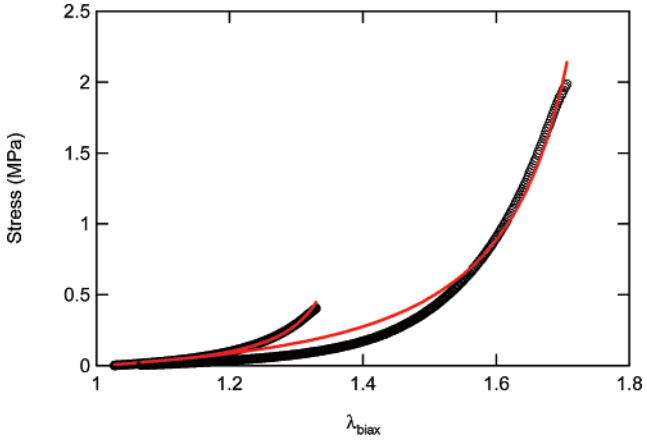

Figure 17. Compressive stress vs biaxial deformation showing the experimental data for two examples of second loading (black markers) and the best fit of the data with Gent's model (thin lines).

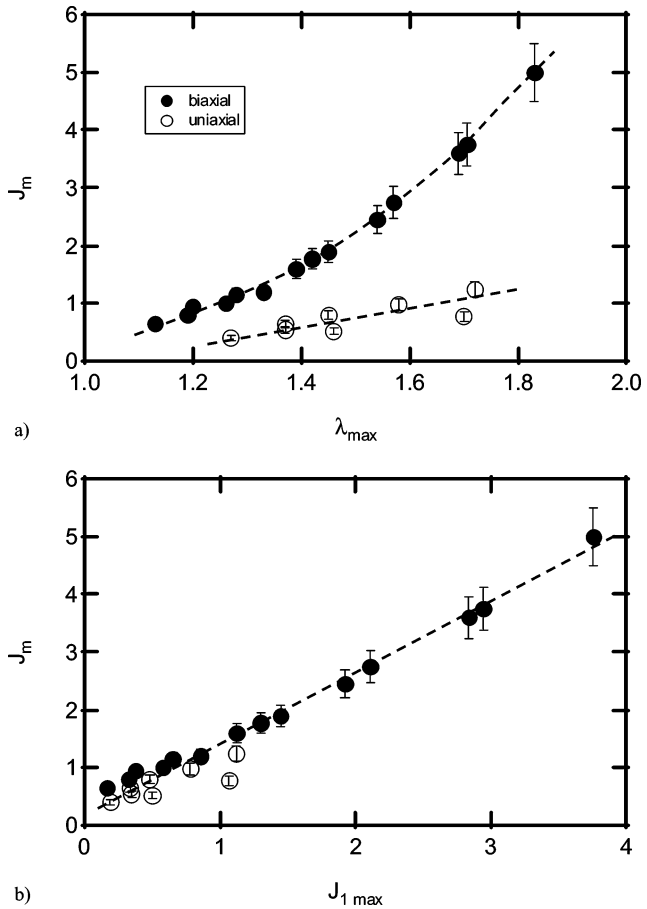

Figure 18. Values of J_m from Gent fits to the DN hydrogel data: (a) as a function of the maximum value of strain achieved during the first loading and (b) as a function of the maximum value of the first strain invariant.

Nevertheless, the G value used in the fit always fell within the range of the experimental small-strain values that were used in Figure 16.

The results of the strain hardening fits are summarized in Figure 18. Interestingly, the correct reduced parameter with which to compare the uniaxial and biaxial data is the maximum value achieved by the first strain invariant rather than the maximum value of the extension as in the discussion on ϕ_b above.

The important result of Figure 18 is that J_m increases markedly with the imposed strain. In other words, the load-

bearing chains becoming available for deformation during the second loading are longer as the $\lambda_{biax,max}$ of the first loading increases, and short chains are being broken. Unlike the fraction of unloaded bonds which only depends on the maximum tensile deformation achieved in the first cycle of loading, the nonlinear elastic properties of the network during the second cycle of loading appear to depend on the maximum value achieved by the first strain invariant during the first cycle.

The reason for this difference is not obvious. It may be due to the different nature of the two parameters. The bonds break when chains reach their full extension, so ϕ_b should be related to the average number of chains per unit volume reaching full extension, i.e., the shortest chains only. On the other hand, J_m is a critical amount of stored energy and should be related to the elastic behavior of the longest chains that are not broken.

Discussion

It is clear from the mechanical data presented in this paper that the behavior of DN gels is very different from that of a regular elastic rubber or a single network gel. As soon as the DN gel is deformed, it undergoes some permanent damage, which then becomes more pronounced as the maximum strain increases. The combined results in tension and compression suggest that the first network of PAMPS is highly heterogeneous in its cross-linking structure and also highly stretched. As soon as it is deformed, some of the shorter strands break and the number of broken strands is a very steep function of λ. The surprising result, however, is that this continuous fracture of bonds does not lead to macroscopic fracture of the material. In other words, no macroscopic crack propagates through the sample although many microscopic, or even molecular, flaws must be created within the material.

Two explanations can be proposed for this failure of crack coalescence, which is the primary reason for the high toughness of this hydrogel material. The first possibility is the bridging effect due to the second network, discussed in the Introduction. It is experimentally clear that the toughening effect is crucially dependent on the existence and nature of the second network. The second network must be neutral, interpenetrate the first network, and either have a very high molecular weight (above 500 kg/mol) or be lightly cross-linked. It should also represent 90% of the weight fraction in polymer. The "crazelike" mechanism proposed by Brown[26] appears a very plausible energy dissipation mechanism that delays macroscopic crack propagation. However, it is also likely that in a situation in which a macroscopic flaw, such as a crack, is present, the stress concentration occurring upon loading is effectively averaged by the softening of the material, even at large distances from the crack tip. In this case, the material essentially forms a very large plasticized zone, with energy dissipation taking place very far from the crack tip in regions where the stress is rather low. This aspect of the toughening mechanism appears similar in principle to what is generally believed to occur in rubber-toughened plastics in which rubber particles act as weak points nucleating cavities, even relatively far from the crack tip, which then act as nucleating points for crazes.[28]

Finally, it is worthwhile to point out that the details of the structure presented in Figure 2 will be highly dependent on the synthesis conditions of the first network. Further investigations with different first network structures may shed some light on the importance of this point for the toughening mechanism.

The other interesting parallel one might draw is between DN gels and the filled elastomer networks used for rubber tires.[29] In these materials, the interactions between polymer and carbon black fillers result in a pronounced first cycle hysteresis that is thought to be responsible for some of the very tough properties observed for these materials.[30] However, in the case of elastomers, the interactions between particles and polymers are not permanently broken, and if the sample is left to rest, it recovers its virgin strength, typically within 30 min. We retested our samples more than a week after the initial trials without recovering much (if any) of the original strength, strongly suggesting that we are indeed seeing irreversible bond fracture during the first loading cycle.

Conclusion

We have demonstrated in this paper that the tough DN gels prepared by the sequential free radical polymerization of AMPS and acrylamide have an extremely heterogeneous cross-link structure with more than 80% of the network strands being very short. As a result, any deformation beyond about 20% results in significant bond fracture in the material as demonstrated by the large hysteresis observed in the first cycle of loading−unloading.

This very large hysteresis is thought to be linked to the high toughness of the gel. To our knowledge, it is the first time that such an energy dissipation mechanism, similar to the Mullins effect observed in filled rubbers, has been observed for polymer gels.

The investigation of the change in elastic properties of the network after the first cycle of mechanical testing reveals interesting information concerning the degree of heterogeneity in the first network, which should be characteristic of the details of the synthesis conditions of that network.

When comparing tests in large strain performed in uniaxial compression (biaxial tension) and uniaxial tension, we found that the fraction of unloaded bonds only depends on the maximum tensile deformation achieved in the first cycle of loading. On the other hand, when the nonlinear elastic properties of the network during the second cycle of loading are analyzed with a constitutive equation, the main parameter controlling the onset of strain hardening in the polymer chains during the second loading cycle appears to be the maximum value achieved by the first strain invariant J_1 during the first cycle.

The type of systematic hysteresis experiments reported in this paper could be used to investigate the degree of heterogeneity of different DN networks in order to better understand which distribution of network strand lengths provides the most efficient toughening of the gel. In this way, a more complete picture of the behavior of these complex and interesting hydrogel materials could be achieved.

References and Notes

(1) Gombotz, W. R.; Wee, S. F. *Adv. Drug Delivery Rev.* **1998**, *31*, 267−285.
(2) Lee, K. Y.; Mooney, D. J. *Chem. Rev.* **2001**, *101*, 1869−1879.
(3) Rowley, J. A.; Madlambayan, G.; Mooney, D. J. *Biomaterials* **1999**, *20*, 45−53.
(4) Chen, J.; Park, H.; Park, K. *J. Biomed. Mater. Res.* **1999**, *44*, 53−62.
(5) Eddington, D. T.; Beebe, D. J. *Adv. Drug Delivery Rev.* **2004**, *56*, 199−210.
(6) Nicolson, P. C.; Vogt, J. *Biomaterials* **2001**, *22*, 3273−3283.
(7) Tanaka, Y.; Gong, J. P.; Osada, Y. *Prog. Polym. Sci.* **2005**, *30*, 1−9.
(8) Gong, J. P.; Katsuyama, Y.; Kurokawa, T.; Osada, Y. *Adv. Mater.* **2003**, *15*, 1155−1158.
(9) Tanaka, Y.; Kuwabara, R.; Na, Y. H.; Kurokawa, T.; Gong, J. P.; Osada, Y. *J. Phys. Chem. B* **2005**, *109*, 11559−11562.
(10) Haraguchi, K.; Li, H. J. *Macromolecules* **2006**, *39*, 1898−1905.
(11) Kong, H. J.; Wong, E.; Mooney, D. J. *Macromolecules* **2003**, *36*, 4582−4588.
(12) Webber, R. E.; Shull, K. R. *Macromolecules* **2004**, *37*, 6153−6160.

(13) Djonlagic, J.; Petrovic, Z. S. *J. Polym. Sci., Part B: Polym. Phys.* **2004**, *42*, 3987−3999.
(14) Gent, A. N. *Rubber Chem. Technol.* **1996**, *69*, 59−61.
(15) Edwards, S. F.; Vilgis, T. A. *Rep. Prog. Phys.* **1988**, *51*, 243−297.
(16) Skouri, R.; Schosseler, F.; Munch, J. P.; Candau, S. J. *Macromolecules* **1995**, *28*, 197−210.
(17) Melekaslan, D.; Okay, O. *Polymer* **2000**, *41*, 5737−5747.
(18) Okay, O.; Sariisik, S. B.; Zor, S. D. *J. Appl. Polym. Sci.* **1998**, *70*, 567−575.
(19) Kizilay, M. Y.; Okay, O. *Macromolecules* **2003**, *36*, 6856−6862.
(20) Tsukeshiba, H.; Huang, M.; Na, Y. H.; Kurokawa, T.; Kuwabara, R.; Tanaka, Y.; Furukawa, H.; Osada, Y.; Gong, J. P. *J. Phys. Chem. B* **2005**, *109*, 16304−16309.
(21) Na, Y. H.; Kurokawa, T.; Katsuyama, Y.; Tsukeshiba, H.; Gong, J. P.; Osada, Y.; Okabe, S.; Karino, T.; Shibayama, M. *Macromolecules* **2004**, *37*, 5370−5374.
(22) Persson, B. N. J.; Brener, E. A. *Phys. Rev. E* **2005**, *71*.
(23) Lake, G. J.; Lindley, P. B. *J. Appl. Polym. Sci.* **1965**, *9*, 1233−1251.
(24) Mendes, E.; Lindner, P.; Buzier, M.; Boue, F.; Bastide, J. *Phys. Rev. Lett.* **1991**, *66*, 1595−1598.
(25) Ozmen, M. M.; Okay, O. *Polym. Bull.* **2004**, *52*, 83−90.
(26) Brown, H. R. *Macromolecules*, in press.
(27) Na, Y. H.; Tanaka, Y.; Kawauchi, Y.; Furukawa, H.; Sumiyoshi, T.; Gong, J. P.; Osada, Y. *Macromolecules* **2006**, *39*, 4641−4645.
(28) Plummer, C. J. G.; Béguelin, P.; Kausch, H.-H. *Colloids Surf., A* **1999**, *153*, 551−566.
(29) Heinrich, G.; Kluppel, M. *Adv. Polym. Sci.* **2002**, *160*, 1−44.
(30) Heinrich, G.; Kluppel, M.; Vilgis, T. A. *Curr. Opin. Solid State Mater. Sci.* **2002**, *6*, 195−203.

MA062924Y